

Inhibition of SCD1 impairs palmitate-derived autophagy at the step of autophagosome-lysosome fusion in pancreatic β -cells^S

Justyna Janikiewicz,* Katarzyna Hanzelka,* Anna Dziewulska,* Kamil Kozinski,* Pawel Dobrzyn,[†] Tytus Bernas,[§] and Agnieszka Dobrzyn^{1,*}

Laboratories of Cell Signaling and Metabolic Disorders,* Medical Molecular Biochemistry,[†] and Functional and Structural Tissue Imaging,[§] Nencki Institute of Experimental Biology, Polish Academy of Sciences, Warsaw, Poland

Abstract Autophagy is indispensable for the proper architecture and flawless functioning of pancreatic β -cells. A growing body of evidence indicates reciprocal communication between autophagic pathways, apoptosis, and intracellular lipids. The way in which elevated levels of free saturated or unsaturated FAs contribute to progressive β -cell failure remains incompletely understood. Stearoyl-CoA desaturase (SCD1), a key regulatory enzyme in biosynthesis of MUFAs, was shown to play an important role in regulation of β -cell function. Here, we investigated whether SCD1 activity is engaged in palmitate-induced pancreatic β -cell autophagy. We found augmented apoptosis and diminished autophagy upon cotreatment of INS-1E cells with palmitate and an SCD1 inhibitor. Furthermore, we found that additional treatment of the cells with monensin, an inhibitor of autophagy at the step of fusion, exacerbates palmitate-induced apoptosis. Accordingly, diminished SCD1 activity affected the accumulation, composition, and saturation status of cellular membrane phospholipids and neutral lipids. Such an effect was accompanied by aberrant endoplasmic reticulum stress, mitochondrial injury, and decreases in insulin secretion and cell proliferation. Our data reveal a novel mechanism by which the inhibition of SCD1 activity affects autophagosome-lysosome fusion because of perturbations in cellular membrane integrity, thus leading to an aberrant stress response and β -cell failure.—Janikiewicz, J., K. Hanzelka, A. Dziewulska, K. Kozinski, P. Dobrzyn, T. Bernas, and A. Dobrzyn. **Inhibition of SCD1 impairs palmitate-derived autophagy at the step of autophagosome-lysosome fusion in pancreatic β -cells.** *J. Lipid Res.* 2015. 56: 1901–1911.

Supplementary key words apoptosis • cardiolipin • diabetes • fatty acid/desaturases • insulin • pancreas • phospholipids

This work was supported by Polish Science Foundation Grant TEAM/2010-5/2 (A.Do.) and National Science Centre Grants UMO 2011/03/B/NZ4/03055 (A.Do.), UMO 2014/13/B/NZ4/00199 (P.D.), UMO 2013/09/B/NZ3/01389 (T.B.), and UMO 2012/05/E/ST2/02180 (T.B.).

Manuscript received 10 April 2015 and in revised form 8 July 2015.

Published, *JLR Papers in Press*, August 20, 2015
DOI 10.1194/jlr.M059980

Elevated levels of FFAs, often accompanied by obesity, have been considered as a major risk factor of β -cell failure and insulin resistance, which contributes to the onset and progression of T2D (1). The FA-induced effect on β -cell integrity and function depends on both the level of FA desaturation and the time of deposition (2). The prolonged exposure of β -cells to high concentrations of FAs results in an impairment in insulin secretion, a decrease in insulin gene expression, the mitigation of proliferation, and subsequently the induction of lipoapoptosis (3). The molecular mechanisms that link FAs to β -cell dysfunction still remain to be delineated. Several processes by which FAs mediate lipotoxicity have been suggested, including the generation of reactive oxygen species, de novo ceramide synthesis, endoplasmic reticulum (ER)-associated stress, and alterations in mitochondrial integrity and function (4–6). Saturated FAs (SFAs) were found to cause more severe effects on the insulin secretory capacity of β -cells and rate of apoptosis compared with MUFAs (7, 8).

Stearoyl-CoA desaturase (SCD) is the pivotal lipid metabolism enzyme that catalyzes the biosynthesis of MUFAs by introducing a *cis*-double bond to a fatty-acyl CoA. The preferred desaturation substrates are palmitic acid (16:0) and stearic acid (18:0), which are converted to palmitoleate (16:1n-7) and oleate (18:1n-9), respectively (9). The resulting

Abbreviations: BrdU, bromodeoxyuridine; ChE, cholesteryl ester; C/EBP, CCAT/enhancer binding protein; CHOP, C/EBP homologous protein; CL, cardiolipin; CQ, chloroquine diphosphate; DAG, diacylglycerol; DAPI, 4',6-diamidino-2-phenylindole; E/P, E64d/pepstatin A; ER, endoplasmic reticulum; KRBB, Krebs-Ringer bicarbonate buffer; LAMP1, lysosome-associated membrane protein 1; LC3B, microtubule-associated protein 1 light chain 3B; 3-MA, 3-methyladenine; MN, monensin; PC, phosphatidylcholine; PE, phosphatidylethanolamine; p-eIF2 α , phospho-eukaryotic translation initiation factor 2 subunit α ; PL, phospholipid; PS, phosphatidylserine; SCD, stearoyl-CoA desaturase; SFA, saturated FA; USFA, unsaturated FA.

¹To whom correspondence should be addressed.

e-mail: adobrzyn@nencki.gov.pl

^SThe online version of this article (available at <http://www.jlr.org>) contains a supplement.

MUFAs are the major components of such complex lipid classes as TGs, diacylglycerols (DAGs), phospholipids (PLs), wax esters, and cholesteryl esters (ChEs). SCD is recognized as a critical enzyme for the structure of cellular membranes, lipid signaling molecules, and energy storage species (10). Much recent attention has been given to SCD1, the major isoform that is expressed in lipogenic tissues, including the liver and adipose tissue. Mice that are deficient in the *SCD1* gene exhibit increases in energy expenditure and insulin sensitivity and a decrease in body adiposity, but are also resistant to diet-induced obesity (11–13). Targeted SCD1 deficiency has the potential to protect against many aspects of metabolic syndrome, but the converse appears to occur for pancreatic β -cells. *SCD1* knockdown in MIN6 or INS-1E cells augmented palmitate-induced apoptosis compared with nontargeted controls (14, 15), whereas an increase in *SCD1* expression and desaturation activity within a subpopulation of palmitate-resistant MIN6 cells was detected (4). Mice on a BTBR *leptin*^{ob/ob} background that lack *SCD1* exhibited a decline in glucose-stimulated insulin secretion, and a subpopulation of β -cells displayed hallmarks of SFA-induced lipotoxicity (16).

Recent reports support the concept that autophagic, apoptotic, and lipid metabolism networks are interrelated within the context of lipotoxicity (17, 18). Macroautophagy (hereinafter referred to as autophagy) is a major intracellular quality control and degradation system by which cells that are under harmful conditions eliminate or recycle impaired organelles and various macromolecules by utilizing lysosomal machinery (19). Basal autophagy is indispensable for maintaining the proper architecture and undisturbed functioning of pancreatic β -cells (20). Mice with autophagy-deficient β -cells exhibited an impairment of glucose tolerance and typical hallmarks of islet failure (21, 22). Furthermore, an increase in autophagosome formation was reported in Zucker diabetic fatty rats (23), *db/db* mice, and C57BL/6 mice that were fed a high-fat diet (22). These studies support the hypothesis that compromised autophagic activity may contribute to β -cell failure and predispose individuals to T2D (24). Pancreatic β -cells from obese human T2D cadavers and the ex vivo exposure of pancreatic islets from rats and nondiabetic individuals to a palmitate/oleate combination resulted in autophagic vacuole overload and an increase in cellular damage (25, 26). Consequently, long-chain FAs are considered the most plausible candidates for triggering perturbations in β -cell autophagy.

Considering that SCD1 is a well-established determinant of intracellular MUFA/SFA equilibrium and manifests a protective action against lipodysfunction in β -cells, we investigated whether SCD1 is involved in FA-induced autophagy/apoptosis crosstalk in pancreatic β -cells. Our findings suggest that a decrease in the activity of SCD1 impairs autophagic flux at the step of fusion with lysosomes. Moreover, such an intervention exacerbates palmitate-induced apoptosis in pancreatic β -cells through a mechanism that involves alterations in the accumulation of distinct PL and neutral lipid classes, in conjunction with changes in FA saturation status in cellular membranes and the induction of ER-to-mitochondria stress signaling.

Materials

Primary antibodies against cleaved caspase 3, caspase 9, binding immunoglobulin protein, phospho-eukaryotic translation initiation factor 2 subunit α (p-eIF2 α), and eIF2 α were obtained from Cell Signaling Technology (Hertfordshire, UK). Anti-microtubule-associated protein 1 light chain 3B (LC3B) and peroxidase-conjugated β -actin antibodies were purchased from Sigma (St. Louis, MO). Antibodies against CCAAT/enhancer binding protein (C/EBP) homologous protein (CHOP) and lysosome-associated membrane protein 1 (LAMP1) were obtained from Santa Cruz Biotechnology (Santa Cruz, CA). Secondary antibodies conjugated with Alexa Fluor-488 and Alexa Fluor-568 were obtained from Life Technologies (Carlsbad, CA). The other chemicals were purchased from Sigma unless otherwise specified.

Cell culture and chronic treatments

The rat insulinoma β -cell line, INS-1E, was a generous gift from Dr. Pierre Maechler (University of Geneva, Geneva, Switzerland) and was maintained in a regular medium as previously described (27). Briefly, the cells were cultured in a 5% CO₂ atmosphere at 37°C in complete RPMI 1640 supplemented with 5% heat-inactivated fetal bovine serum, 1 mM sodium pyruvate, 50 μ M 2-mercaptoethanol, 2 mM glutamine, 10 mM HEPES, 100 U/ml penicillin, and 100 μ g/ml streptomycin. To verify the effects of SCD1 inhibition on autophagy, apoptosis, proliferation, insulin secretion, and subcellular fractionation, the cells were preincubated with 2 μ M of the SCD1 inhibitor, A939572 (Biofine International, Blain, WA), for 4 h and then cosupplemented with 0.4 mM palmitic acid-BSA conjugate for 16 h. To silence SCD1 expression, 60 ng of siRNA against SCD1 (s73339) from Ambion (Houston, TX) was used. Silencer Negative Control #1 siRNA (Ambion) was employed as a negative control. The reverse transfection of INS-1E cells was performed using Lipofectamine 2000 (0.5 μ l/cm²; Life Technologies). The silencing efficiency was measured 72 h after transfection using real-time PCR and Western blot. Palmitic acid was added for the last 16 h prior to sample collection. The enzymatic activity of SCD1, after administration of SCD1 inhibitor or siRNA, was analyzed by calculating the desaturation index as described below. To analyze the engagement of SCD1 in particular stages of autophagy and for confocal microscopy, INS-1E cells were pretreated with 2 μ M of the SCD1 inhibitor for 3 h and then cosupplemented with one of the following autophagy inhibitors for 1 h: 3-methyladenine (3-MA; 5 mM), monensin (MN) sodium (80 nM), chloroquine diphosphate (CQ; 25 μ M), or E64d/pepstatin A (E/P; 10 μ g/ml). Afterward, 0.4 mM palmitate was added for 16 h to the culture medium, which already contained the SCD1 inhibitor and one of the inhibitors of autophagy mentioned above. For all of the experiments, control cells for palmitate treatment were INS-1E cells that were incubated in medium supplemented with a 7.5% BSA. DMSO, water, or ethanol was used as a vehicle control for the aforementioned SCD1 and autophagy inhibitors, respectively.

Isolation and analysis of RNA

Total RNA was isolated from INS-1E cells using TRIzol reagent (Life Technologies). DNase-treated RNA was reverse-transcribed with SuperScript III (Life Technologies), and real-time quantitative PCR was performed on an ABI Prism 7900 HT Fast instrument. Fast SYBR green (Thermo Scientific, Pittsburgh, PA) was used for the detection and quantification of genes that were expressed as mRNA, and the level was normalized to β -actin using the $\Delta\Delta$ Ct method.

Western blot

Cells were collected and lysed for 30 min in ice-cold buffer [50 mM Tris-HCl (pH 7.4), 5 mM EDTA, 1% Triton X-100, and

150 mM NaCl] that contained protease (10 $\mu\text{g}/\mu\text{l}$ leupeptin, 5 $\mu\text{g}/\mu\text{l}$ pepstatin A, 2 $\mu\text{g}/\mu\text{l}$ aprotinin, and 1 mM phenylmethylsulfonyl fluoride) and phosphatase (1 mM sodium orthovanadate and 10 mM sodium fluoride) inhibitors. After centrifugation at 12,000 g at 4°C for 15 min, the supernatants were used as whole-cell lysates for further analyses. The protein content was determined using the Bio-Rad protein assay (Bio-Rad, Hercules, CA) with BSA as the standard. An equal amount of each protein sample was resolved by sodium dodecyl sulfate-polyacrylamide gel electrophoresis and transferred to polyvinylidene difluoride membranes (Millipore, Billerica, MA). After blocking with 5% nonfat milk, membranes were probed with appropriate primary and horseradish peroxidase-conjugated secondary antibodies, respectively. Bands were visualized using Chemiluminescence HR substrate reagent (Millipore).

Glucose-stimulated insulin secretion

INS-1E cells were preincubated for 1 h in Krebs-Ringer bicarbonate buffer (KRBB) that contained 2.75 mM glucose. Subsequently, KRBB was replaced with 500 μl of the same buffer or 500 μl of fresh KRBB supplemented with 16.5 mM glucose. After incubation for an additional 1 h, the replenished buffers above the cells were collected to measure basal and glucose-stimulated insulin release. INS-1E cells from corresponding wells were lysed, and the protein content was measured as described above. The insulin concentration in the acquired buffers was determined using the Rat/Mouse Insulin ELISA kit (Millipore) according to the manufacturer's instructions.

Cell proliferation

INS-1E cells were seeded in 24-well plates at 3×10^5 cells/well and subjected to the above treatments. Bromodeoxyuridine (BrdU) solution (10 μM) was then added, and the cells were incubated for 2 h. BrdU incorporation into DNA was measured using the cell proliferation ELISA BrdU colorimetric kit (Roche Diagnostics, Penzberg, Germany) according to the manufacturer's recommendations.

Confocal microscopy

INS-1E cells were grown on 0.001% poly-L-ornithine-precoated coverslips in 24-well plates. The cells were washed with PBS and then fixed with 4% paraformaldehyde for 15 min at room temperature. Fixed cells were subsequently permeabilized with 0.2% Tween-20 for 10 min, rinsed twice with PBS, and blocked with buffer that consisted of 3% BSA in PBS for 45 min. Primary antibodies for LAMP1 (Alexa 488) were applied in blocking buffer overnight. The next day, at the end of the treatment, anti-LC3B (Alexa 561) antibody was coadministered for an additional 1 h to obtain dual immunostaining. INS-1E cells were then washed three times in PBS and exposed to appropriate fluorescently labeled secondary antibody for 1 h. After additional rinses, the cells were costained with 4',6-diamidino-2-phenylindole (DAPI) for nucleus identification. Fluorescence 3D images were acquired (Nyquist sampling) using a Leica SP8 confocal microscope with a 63 \times oil objective (NA = 1.4), segmented, and analyzed using Matlab 2013a. At least three randomly selected optical fields with at least 15–20 cells within each field were collected in triplicate for each experimental condition. Prior to segmentation, the stacks of optical sections (Alexa 488 and 568) were subjected to blind deconvolution (15 iterations) using Huygens v. 3.7 (SVI Imaging, Hilversum, The Netherlands). Processing was initiated with nominal point spread function of the objective and performed with the signal-to-noise ratio set to 15. The background was estimated as a minimum of the average intensity in a 25 \times 25 region. Following deconvolution, the nuclei (DAPI) were segmented using Otsu thresholding (two classes).

Overlapping nuclei were separated by Euclidean distance transform followed by watershedding. The Alexa 488 and 568 images were summed, processed with a median filter (size 7 \times 7 \times 3) and dilated (10 \times 10 \times 3 neighborhood). The cells were segmented using Otsu thresholding, and single-cell masks were constructed with iterative dilation of the nuclear masks. The dilation steps were ordered by the intensity of processed cell images. The volumes that corresponded to nuclei were then excluded from the cell masks. The background of deconvolved images (Alexa 488 and 568) was estimated using gray-scale erosion (10 \times 10 \times 3 neighborhood) that was subtracted from the original (deconvolved) data. The Spearman coefficient of the intensity correlation between the intensities of the Alexa 488 and 568 images was calculated on a cell-by-cell basis using the respective masks. The operation was repeated using Alexa 568 images that were shifted by ± 8 voxels in the x and y directions and ± 2 voxels in the z direction. The respective coefficients were calculated using the union of two respective cellular masks and corresponded to the random association of Alexa 488 and 568 fluorescence in a cell. The raw correlation coefficients were then divided by their random counterparts on a cell-by-cell basis to create standardized Spearman values.

Subcellular fractionation

Cells were scraped in ice-cold PBS and centrifuged at 800 g for 5 min to pellet the cells. The pellets were then homogenized in buffer [20 mM Tris-HCl (pH 7.5), 0.5 mM EDTA, 0.5 mM ethylene glycol tetraacetic acid, 10 mM β -mercaptoethanol, 1 mM phenylmethylsulfonyl fluoride, 1 mM Na_3VO_4 , 10 mM NaF, 10 $\mu\text{g}/\mu\text{l}$ leupeptin, 5 $\mu\text{g}/\mu\text{l}$ pepstatin A, and 2 $\mu\text{g}/\mu\text{l}$ aprotinin] through cycles of vortexing, snap-freezing in liquid nitrogen, and shearing through a 25 gauge needle on ice. The lysate was centrifuged at 100,000 g for 1 h at 4°C, and the supernatant that represented the cytosolic fraction was transferred to a fresh tube. The pellet (crude membrane fraction) was either subjected to a lipid extraction procedure or stored at -80°C for further processing. On such occasions, the pellet was resuspended in homogenizing buffer supplemented with 0.5% Triton X-100, passed through a 25 gauge needle on ice, and centrifuged at 18,000 g for 15 min at 4°C to remove insoluble material. The remaining supernatant was established as the membrane fraction. The resulting fractions were subjected to the evaluation of protein content and characterized for organelle markers via immunoblotting (data not shown).

Lipid analysis

Lipids were extracted using the Bligh and Dyer method (28), and separated on silica thin-layer chromatography plates with *n*-heptane/isopropyl ether/glacial acetic acid (60/40/3, v/v/v) for neutral lipids or chloroform/methanol/acetic acid/water (50/37.5/3.5/2, v/v/v/v) for PLs. Bands were then visualized with 0.2% 2,3-dichlorofluorescein, scraped off, and transmethylated in the presence of 14% boron trifluoride in methanol. Subsequently, the resulting FA methyl esters were extracted with hexane and subjected to GC-MS using an Agilent 7890A-5975C GC-MS system (Agilent Technologies, Santa Clara, CA) that was equipped with an Agilent 19091N-205 capillary column. Nonadecanoic acid was used as an internal standard. Mass-to-charge ratios of the FA methyl esters were determined by selected ion monitoring.

Desaturation index

The content of palmitoleic acid (16:1n-7), palmitic acid (16:0), oleic acid (18:1n9), and stearic acid (18:0) in total lipid extracts was analyzed by GC-MS, as described above, and used to calculate the 16:1n7/16:0 and 18:1n9/18:0 ratios.

Statistical analysis

The data are expressed as mean \pm SD. A two-sided *t*-test was applied when differences between two groups were analyzed. Multiple comparisons were performed using one-way ANOVA followed by Dunnett's or Tukey's post hoc test, respectively, using Prism 6.04 software (GraphPad Software, La Jolla, CA). The level of significance was $P < 0.05$.

RESULTS

Palmitate increases apoptosis and autophagy in INS-1E cells

Palmitic acid upregulates apoptosis and autophagy in numerous cell types, including cultured hepatocytes and endothelial cells (29, 30). To examine whether palmitate-induced apoptosis and autophagy occur in pancreatic β -cells, we treated INS-1E cells with 0.4 mM palmitate at consecutive time points. The incubation of INS-1E with palmitate for 8 h was sufficient to increase the cleavage of caspase 3, suggesting the initiation of apoptosis (Fig. 1A). The activation of autophagy by palmitate was analyzed by immunoblotting the lipidated endogenous form of LC3B II. LC3B II is specifically associated with mature autophagosomes, and its levels correlate with the number of autophagosomes until it is degraded by lysosomal machinery (31). An increase in the level of LC3B II, indicating the induction of autophagy, was detected after 6 h exposure of INS-1E cells to 0.4 mM palmitate, which peaked at 16 h and decreased until 24 h (Fig. 1B), compared with the corresponding BSA controls. This effect was further enhanced upon the addition of CQ, a compound that potently impairs lysosomal acidification and blocks the degradation step of autophagy (32), suggesting that palmitate-induced autophagic flux is effective until 16 h (Fig. 1B).

Palmitate-induced autophagy and apoptosis are linked to SCD1 activity

An increase in SCD1 expression was reported to protect pancreatic β -cells from lipid-induced apoptosis (4).

To investigate the impact of SCD1 activity on the palmitate-induced autophagy/apoptosis association, we treated INS-1E cells with the pharmacological SCD1 inhibitor, A939572 (33), which decreased SCD1 activity (expressed as the desaturation index) by $>30\%$ (Fig. 2A). This effect was followed by a 40% decline in LC3B II abundance when INS-1E cells were cotreated with palmitate, suggesting an impairment of autophagy outcome (Fig. 2B). We found that the palmitate-induced cleavage of caspase 3 was elevated more than 2-fold when INS-1E cells were treated with the SCD1 inhibitor (Fig. 2B). In order to confirm the data obtained from chemical SCD1 inhibitor on palmitate-induced autophagy and apoptosis, a transient silencing of SCD1 expression using siRNA was performed. Transfection of INS-1E cells with specific siRNA led to a reduction in SCD1 mRNA and protein levels by over 60 and 90%, respectively (Fig. 2C, D). The SCD1 desaturation ratio indicated more than 60% reduction of the enzyme activity (Fig. 2E). Gene ablation of SCD1 using siRNA had similar effects on palmitate-induced autophagy and apoptosis as SCD1 inhibitor (Fig. 2F), proving that the observed effect is specific for SCD1 downregulation. These results indicate that SCD1 tempers with autophagy in INS-1E cells and simultaneously affects the outcome of palmitate-induced cell death.

Inhibition of SCD1 activity affects autophagic flux at the step of autophagosome-lysosome fusion

To further test the effect of SCD1 inhibition on the level of palmitate-induced autophagic flux and verify which step of autophagy is affected by SCD1, we used pharmacological inhibitors of different stages of autophagy. The levels of autophagic (LC3B II) and apoptotic (cleaved forms of caspase 3) effectors were measured. The treatment of INS-1E cells with 3-MA (an inhibitor of autophagosome formation) increased LC3B II levels in both BSA- and 16:0-treated INS-1E cells (Fig. 3A). This effect was not abolished by the SCD1 inhibitor, suggesting that the initiation of autophagy is unaffected by SCD1 inhibition. Interestingly, an increase in apoptosis was observed after adding the SCD1 inhibitor to INS-1E cells that were incubated with palmitate, but this effect was diminished

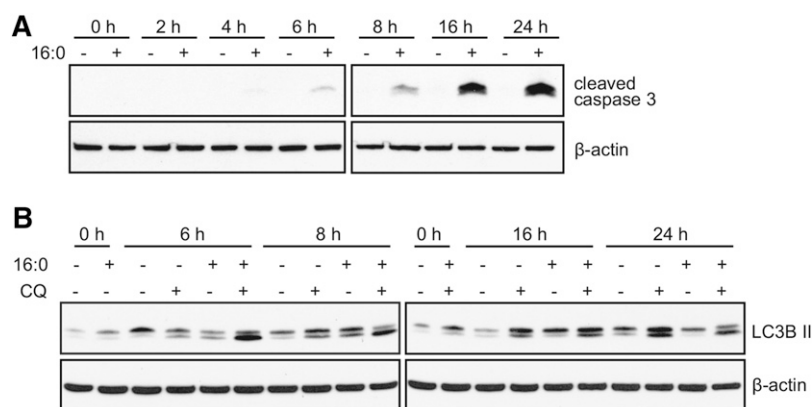


Fig. 1. Palmitate induces apoptosis and autophagy in β -cells. INS-1E cells were treated with 0.4 mM palmitate. A: The level of cleaved caspase 3 was verified by Western blot. B: Autophagic flux was determined by measuring changes in LC3B II levels in the presence of the lysosomal inhibitor, CQ.

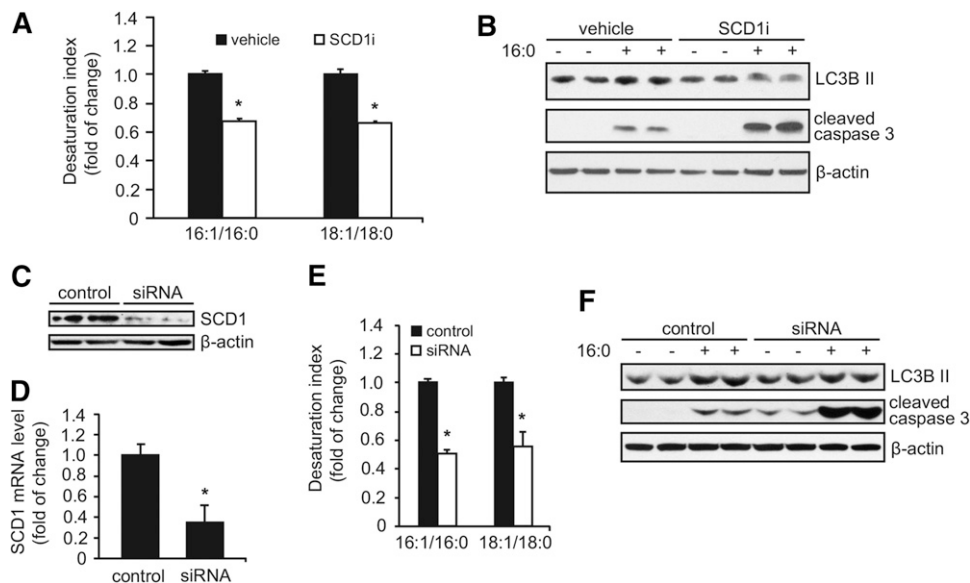


Fig. 2. SCD1 inhibition decreases palmitate-induced autophagy. The desaturation ratio was calculated from the concentrations of 16:1n7 and 16:0 FAs and 18:1n9 and 18:0 FAs in total lipid extracts to evaluate SCD1 activity after treating INS-1E cells with 2 μ M of the SCD1 inhibitor (SCD1i) for 20 h (A) or 72 h after SCD1 silencing (E). B: β -Cells were preincubated in the presence of 2 μ M of the SCD1 inhibitor for 4 h and then treated with BSA or 0.4 mM palmitate for additional 16 h. Alternatively, INS-1E cells were transfected with siRNA specific for SCD1. The silencing efficiency was measured by Western Blot (C) and real-time PCR (D) 72 h after transfection. F: BSA or 0.4 mM palmitate was added for the final 16 h prior to sample collection. The levels of LC3B II and cleaved caspase 3 were analyzed by Western blot. The data are expressed as mean \pm SD (n = 3). * P < 0.05 versus vehicle.

upon the application of 3-MA (Fig. 3A). To determine whether SCD1 might interfere with fusion between autophagosomes and lysosomes, MN (an inhibitor of the aforementioned step) was used. The application of MN together with the SCD1 inhibitor decreased the accumulation of LC3B II, indicating a disturbance in autophagic flux (Fig. 3B). Concomitantly, an increase in the cleavage of caspase 3 was observed upon SCD1 inhibition, and this effect was further enhanced for caspase 3 by the addition of MN (Fig. 3B). Next, we examined E/P, inhibitors of lysosomal proteases, which were applied to block the late stage of autophagy. The treatment of INS-1E cells with E/P and the SCD1 inhibitor exerted a similar effect for LC3B II and apoptotic effectors, similar to the observations in β -cells with inhibited autophagosome-lysosome fusion, suggesting that SCD1 governs the step before autophagosome degradation (Fig. 3C).

Inhibition of SCD1 activity impairs the assemblage between autophagosomes and lysosomes

To further test the hypothesis that SCD1 is engaged in the completion of autophagic flux at the step of fusion, autophagosome and lysosome assemblage was assessed by confocal microscopy using fluorescently labeled LC3B and LAMP1, markers of the aforementioned organelles. A reduction of SCD1 activity led to a significant decline of dual LC3B- and LAMP1-labeled autophagolysosomes in palmitate-treated INS-1E cells (Fig. 4A, B). However, the addition of MN reduced this effect, as confirmed by the Spearman coefficient of the intensity correlation between LC3B and LAMP1 (Fig. 4B), suggesting the blockade of autophagolysosome formation. Moreover, DAPI staining

in INS-1E cells that were incubated with palmitic acid and the SCD1 inhibitor revealed more severe nuclear condensation and blebbing (i.e., typical characteristics of apoptosis) compared with cells that were treated with palmitate alone (Fig. 4A). This effect was consistent with the increase in caspase 3 cleavage upon SCD1 inhibition (Fig. 3B).

Ablation of SCD1 activity affects the composition and content of membrane PLs

PLs are the primary mediators of the autophagic pathway, during which major lipid signaling molecules and cell membrane constituents like phosphatidylinositol, phosphatidylcholine (PC), phosphatidylethanolamine (PE), and phosphatidylserine (PS) mobilize phagophore assembly, conjugate with LC3B on mature autophagosomes (34), and facilitate the merger of autophagosomes with lysosomes (35). To further determine the potential functional relationship between a decrease in SCD1 activity and autophagosome-lysosome fusion, we examined whether changes in the levels of membrane PLs are linked to the aforementioned effects. Intracellular membranes were isolated and subjected to lipid extraction. The SCD1 inhibitor significantly increased the content of PE, PS, and PC in the membranes of control and palmitate-treated INS-1E cells (Fig. 5A). Additionally, SCD1 inhibition in palmitate-treated cells increased the accumulation of cardiolipin (CL) more than 2-fold. Next, we evaluated whether diminished SCD1 activity affects the unsaturated FA (USFA)-to-SFA ratio in cellular membranes of INS-1E cells. The greatest differences were observed with CL, in which SCD1 inhibition or palmitic acid treatment significantly increased

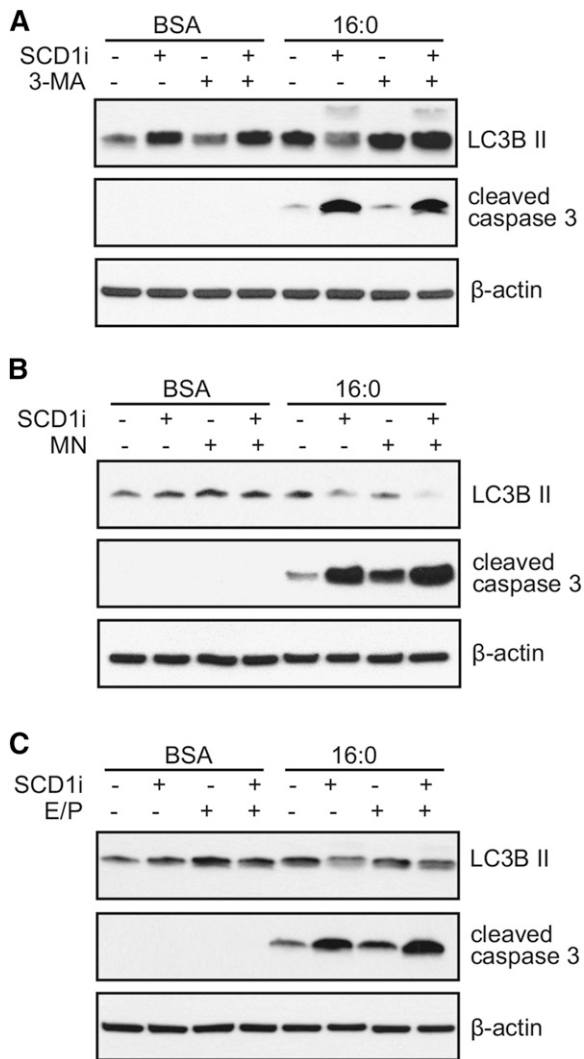


Fig. 3. SCD1 inhibition affects autophagic flux at the step of fusion and lipopoptosis outcome in palmitate-treated INS-1E cells. INS-1E cells with or without SCD1 inhibition were pretreated for 1 h with autophagic inhibitors, 5 mM 3-MA (A), 80 nM MN (B), and 10 μ g/ml E/P (C), followed by incubation with BSA or 0.4 mM palmitate for 16 h. Cleaved caspase 3 and LC3B II levels were measured by Western blot. SCD1i, SCD1 inhibitor.

the USFA/SFA ratio, although cosupplementation with both agents markedly exacerbated this effect (Fig. 5B). For PS, we found that SCD1 inhibition significantly decreased USFA content in both the BSA- and palmitate-treated groups (Fig. 5B). Considering that PC and PE constitute the most abundant PLs of biological membranes (36), we focused on determining the PC/PE ratio, the disequilibrium of which affects membrane integrity. A significant 28% reduction of the PC/PE ratio was observed in INS-1E cells that were cosupplemented with the SCD1 inhibitor and palmitic acid (Fig. 5C). TGs and DAGs are precursors of PL synthesis and the major lipid classes that are stored in cells after FA challenge (37). Importantly, changes in PL content were accompanied by over 6- and 10-fold increases in DAG and FA content, respectively, in INS-1E cells upon cotreatment of the SCD1 inhibitor and palmitate compared with the BSA control or cells that were treated only with palmitate

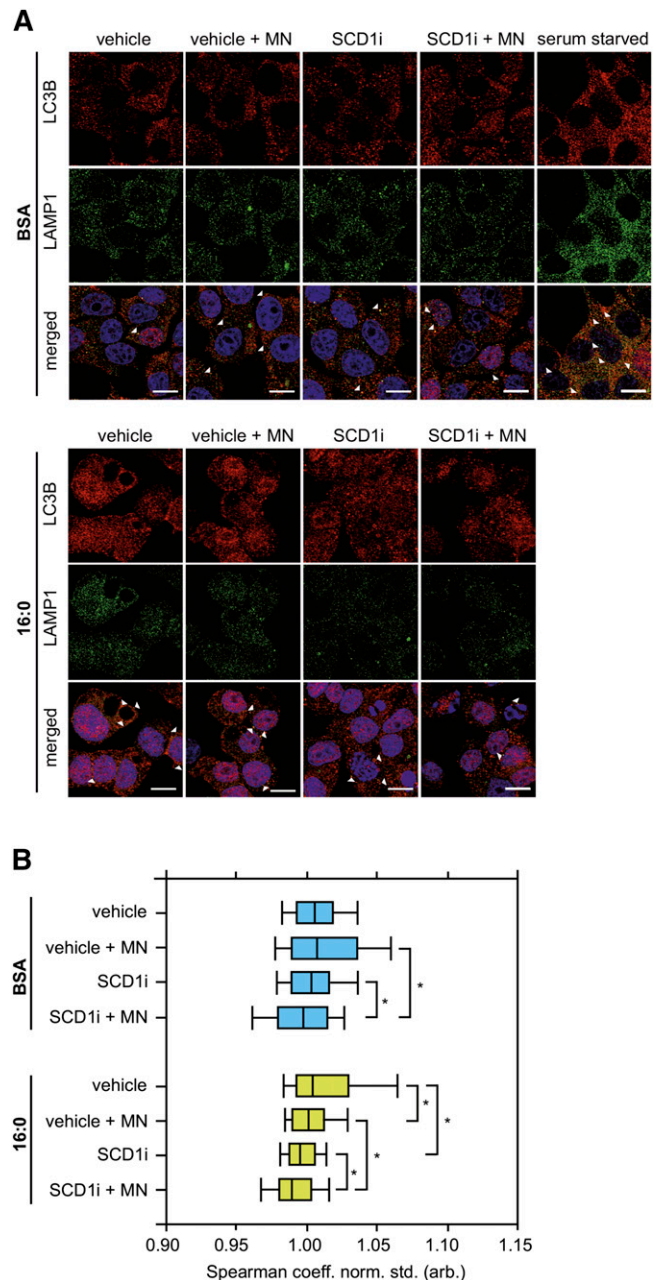


Fig. 4. Lysosomal fusion is impaired in INS-1E cells with SCD1 inhibition. The maturation of autophagosomes into autolysosomes was analyzed in INS-1E cells that were subjected to incubation with 2 μ M of the SCD1 inhibitor (SCDi) and subsequently cotreated with 80 nM MN and/or 0.4 mM palmitate for 16 h. Serum-starved cells were used as a positive control. A: The cells were fixed and stained with DAPI (blue), anti-LC3B (red), and anti-LAMP1 (green) antibodies. Scale bar = 10 μ m. B: Quantification of the colocalization between LC3B and LAMP1, displayed as the Spearman coefficient normalized to vehicle BSA group. * P < 0.05.

(Fig. 5D). In contrast, the relative levels of TGs and ChEs decreased by 21 and 19%, respectively, in this group (Fig. 5D).

Autophagy-associated INS-1E response to SCD1 inhibition depends on ER stress failure and the activation of intrinsic apoptosis

Mitochondria and the ER are cell membrane-derived systems. Their proper functioning relies on their recycling via

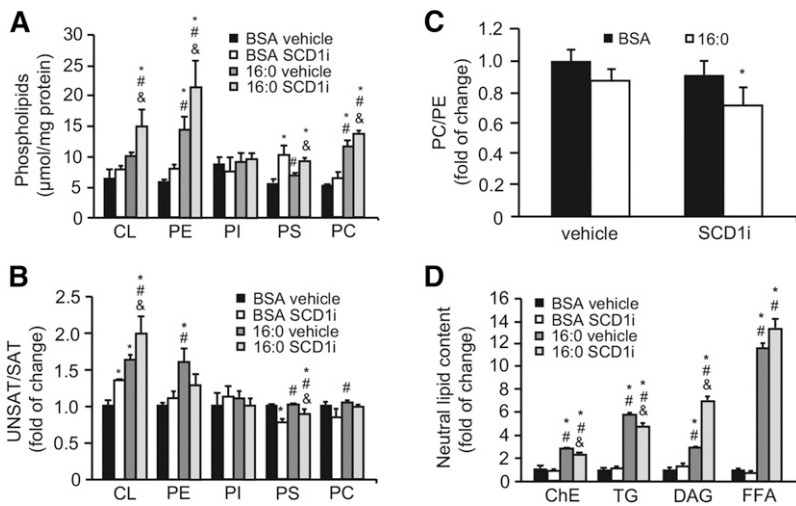


Fig. 5. Decreased SCD1 activity changes the content and composition of membrane PLs and neutral lipids. INS-1E cells were treated with 2 μ M of the SCD1 inhibitor (SCDi), 0.4 mM palmitate, or both and subjected to lipid extraction either from the intracellular membrane fraction or directly from intact cells. Neutral lipids and PLs were extracted from the intact cells and isolated intracellular membrane fraction, respectively, and then separated using thin-layer chromatography and quantified by GC-MS as described in the Materials and Methods. PI, phosphatidylinositol. The data are expressed as mean \pm SD (n = 3). **P* < 0.05 versus BSA vehicle; #*P* < 0.05 versus BSA SCD1 inhibitor; and &*P* < 0.05 versus 16:0 vehicle.

autophagy (19). The highly abundant PLs that are found in mitochondria and the ER are CL, PE, and PC. Our data showed alterations in the PC/PE ratio and a significant increase in the USFA/SFA ratio in CL (Fig. 5), which might affect cellular susceptibility to lipid-induced damage and apoptosis. We further investigated effectors of ER stress and mitochondria-associated cell death. The ER stress markers, CHOP, BiP, and p-eIF2 α , were elevated by 45 and 67%, 50 and 32%, and >30%, respectively, upon independent exposure to palmitate or the SCD1 inhibitor (Fig. 6A). In contrast, the combination of both palmitate and the SCD1 inhibitor decreased the levels of the aforementioned ER stress effectors, suggesting diminished ER stress capacity. We then examined the levels of cleaved caspase 9, which was also elevated to the highest extent in the group that was subjected to both the SCD1 inhibitor and palmitate (Fig. 6B), indicating the activation of mitochondria-associated cell death.

Reduced SCD1 activity deteriorates INS-1E function

Either compromised autophagy or an ineffective ER stress response upon SFA exposure causes the loss of β -cell function (5). To determine how SCD1 inhibition affects β -cell function, INS-1E cells that were subjected to SCD1 inhibition alone or both SCD1 inhibition and palmitate treatment were investigated for glucose-stimulated insulin secretion and proliferation. SCD1 inhibition significantly reduced the secretory response of β -cells to high glucose by 20% compared with control INS-1E cells (Fig. 7A). As expected, prolonged treatment with palmitic acid led to a 55% increase in basal insulin secretion, but decreased the response to high-glucose stimulation by 38% compared with BSA controls. Interestingly, the coincubation of INS-1E cells with the SCD1 inhibitor and palmitate further reduced insulin release at high glucose concentrations, suggesting that their secretory capacity was markedly disrupted (Fig. 7A). This effect was followed by a 70% decline in the rate of proliferation (Fig. 7B).

DISCUSSION

Obesity-related T2D is associated with enhanced autophagy. Recent in vitro and in vivo evidence suggests that

the increase in autophagosome machinery in FA-induced pancreatic failure reflects an impairment of autophagic flux (22, 23, 25). Consequently, a reduction of the autophagic clearance of lipids results in their further accumulation, with detrimental effects on cell survival (17). In the present study, we showed that SCD1 inhibition disturbed autophagic flux at the step of fusion with lysosomes and concomitantly enhanced palmitate-induced β -cell dysfunction and apoptosis. Our study revealed that the mechanisms that link SCD1 inhibition and autophagy/apoptosis crosstalk involve changes in intracellular membrane PLs and the induction of ER-to-mitochondria stress signaling.

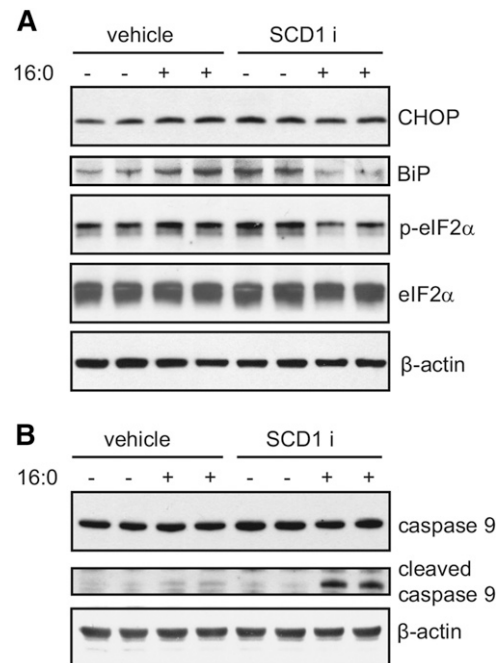


Fig. 6. SCD1 inhibition and palmitate treatment jointly restrain ER stress and trigger mitochondrial injury in INS-1E cells. Whole-cell lysates were collected from INS-1E cells after treatment with the SCD1 inhibitor (SCDi) and palmitic acid. Lysates were then subjected to immunoblotting with antibodies against CHOP, BiP, p-eIF2 α , and eIF2 α for ER stress detection, and cleaved caspase 9 for mitochondrial failure examination.

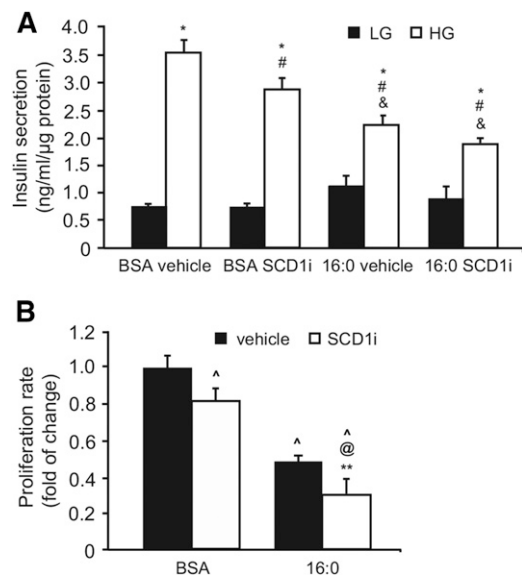


Fig. 7. SCD1 inhibition affects insulin secretion and proliferation rate of INS-1E cells. **A:** After treatment with the SCD1 inhibitor (SCDi) or palmitic acid, INS-1E cells were incubated in the presence of 2.75 mM glucose [low glucose (LG)] or 16.5 mM glucose [high glucose (HG)] for 1 h. The data are expressed as mean \pm SD ($n = 3$). * $P < 0.05$ versus LG; # $P < 0.05$ versus BSA vehicle HG; & $P < 0.05$ versus BSA SCD1i HG. **B:** The proliferation rate of INS-1E cells was measured by BrdU incorporation into DNA of the dividing cells. The data are expressed as mean \pm SD ($n = 3$). ^ $P < 0.05$ versus BSA vehicle; @ $P < 0.05$ versus BSA SCD1i; ** $P < 0.05$ versus 16:0 vehicle.

While SCD1 has been recently shown to be involved in the regulation of starvation-induced autophagy in mouse embryonic fibroblasts (38), the study presented herein is the first time, to our knowledge, that SCD1 is interconnected with palmitate-induced autophagy.

SCD1 plays an important role in β -cell metabolism and survival. In the present study, an increase in palmitate-induced apoptotic cell death was observed in INS-1E cells that were treated with the SCD1 inhibitor, which is consistent with other studies. The genetic ablation of SCD1 in MIN6 and INS-1E cells potentiated palmitate-induced apoptosis (14, 15). A 3-fold increase in *SCD1* expression was detected in a subpopulation of palmitate-resistant MIN6 cells (4). The induced expression of *SCD1* mRNA has been linked to protection against lipotoxicity (39–41). The present study showed, in addition to the effects of palmitate on apoptosis outcome, that SCD1 inhibition led to disrupted autophagy response, demonstrating the existence of crosstalk between the two biological fates in β -cells. This is supported by the recent finding that mouse embryonic fibroblasts with constitutively activated mammalian target of rapamycin complex 1 that were subjected to SCD1 deficiency exhibited an impairment in de novo lipogenesis and the induction of transcription of forkhead box protein O1-dependent autophagy genes (38). Furthermore, oleic acid that is produced by SCD1 was shown to be required for starvation-induced autophagy in mouse embryonic fibroblasts (42).

For complete autophagy maturation, autophagosomes need to fuse with lysosomes and form autophagolysosomes,

with degradation of the engulfed cargo (17, 43). We showed an increase in LC3B II level in the presence of the autophagosome formation inhibitor 3-MA in the presence or absence of BSA. This result is opposite to the one reported by Choi et al. (44), who observed that 3-MA reduces LC3B II level in palmitate-treated INS-1E cells. However, in the study by Choi et al. (44), INS-1E cells were treated with palmitate together with high glucose, thus it refers to glucolipotoxicity rather than to lipotoxic effect on β -cells, as it is in our study. Increased levels of LC3B II can result from either increased synthesis of autophagosomes or reduced autophagosome turnover (31). In contrast, diminished levels of LC3B II are not only associated with a drop in autophagosome synthesis, but also with a very rapid lysosomal turnover (45, 46). Because we observed a decrease in the level of LC3B II in INS-1E cells treated with SCD1 inhibitor alone or with addition of palmitate, we anticipated the impairment of autophagic flux at later steps. We further investigated which of the autophagy stages is affected by diminished SCD1 activity by using autophagy inhibitors: 3MA, MN, and E/P. In the presence of such agents, accumulation of LC3B II supports the idea of efficient autophagic flux, whereas the opposite result indicates a defect or delay in the process, prior lysosomal degradation (31). The induction of autophagy by prolonged treatment with 3-MA in nutrient-rich conditions was already shown in HeLa and HEK293T cells (47). Conversely, an SCD1 inhibitor treatment exerts a reduction or no change in the levels of LC3B II in the absence or presence of MN and E/P, respectively, thus indicating on inefficient flux at later stages and worse apoptosis outcome. The impairment of fusion between autophagosomes and lysosomes was also confirmed by confocal microscopy, where INS-1E cells subjected to SCD1 inhibition and palmitate treatment showed a significant reduction in dual LC3B- and LAMP1-labeled autophagolysosomes. Therefore, our study provides evidence that SCD1 tempers with autophagy outcome at the step of autophagolysosome formation. Previous studies indicated that changes in the lipid composition of autophagosomal or lysosomal membranes potentially modify their fusogenic capacity because of altered cholesterol content (35). Modifications of SFA and USFA composition in intracellular PLs might affect membrane properties (36) and potentially influence autophagic flux. Our study supports this possibility, given that SCD1 inhibition resulted in significant changes in membrane PL composition. The greatest differences in abundance and saturation status were found among PS, PC, PE, and CL. These findings correlate well with our previous study, which showed that SCD1 deficiency regulates PE and PC biosynthesis (48). Mice that lack SCD1 exhibit an increase in PUFA-rich PL content and, consequently, alterations in plasma membrane fluidity in the liver (48). Therefore, one proposed mechanism that drives the impairment of autophagosome-lysosome fusion that is caused by SCD1 inhibition in pancreatic β -cells might be associated with changes in membrane PL saturation status.

Autophagy is widely accepted to be essential for pancreatic β -cell function and survival (20), and palmitate-induced

autophagy might protect against lipotoxicity (49). Based on the increase in the relative abundance of PL moieties associated with SCD1 inhibition and considering that TGs together with DAGs are both precursors of PLs and major lipid classes that are stored in cells after FA challenge (37), we postulated that the accumulation of neutral lipids might be affected in pancreatic β -cells treated with an SCD1 inhibitor. Indeed, palmitate treatment significantly increased ChE, TG, DAG, and FFA content in INS-1E cells, and SCD1 inhibition reduced ChE and TG accumulation and simultaneously increased DAGs and FFAs. The deposition of TGs in lipid droplets is recognized as being more protective than products of their lipolysis or lipid intermediates of TG synthesis that harm β -cell viability (37, 50). Furthermore, the blockade of SCD1 activity inhibited ChE formation in palmitate-resistant MIN6 cells and restored their susceptibility to lipoapoptosis (4). In the present study, we observed the presence of extensive lipid droplets in individual palmitate-treated INS-1E cells, but the addition of the SCD1 inhibitor decreased the size and number of droplets per single cell (data not shown). This finding coincided with a decline in the relative amounts of TGs and ChEs, essential components of the lipid droplet core (50). Similarly, the genetic inhibition of SCD1 in INS-1E cells decreased palmitate incorporation into TGs and ChEs, with the simultaneous accumulation of DAGs (15). We speculate that during prolonged palmitate treatment, when the lipid storage capacity is compromised, the lack of SCD1 activity results in the channeling of TGs into more deleterious DAGs, thus exacerbating the adverse effects on apoptosis and autophagy. This is followed by the impairment of pancreatic β -cell function, reflected by reductions of insulin secretion and proliferation rate in INS-1E cells that are subjected to SCD1 inhibition.

The ER is considered to be the main site of lipid synthesis, membrane biogenesis, and calcium storage. However, any disturbance in ER homeostasis drives cellular stress and activates the unfolded protein response (5). In the present study, the independent treatment of INS-1E cells with either the SCD1 inhibitor or palmitate triggered the induction of ER stress markers. The ability of palmitate to induce ER stress in cultured cells is intertwined with its incorporation into the ER membrane (51). A subsequent increase in ER PL saturation status was reported to be a potent factor that compromises its structure and integrity (52–55). In the present study, combined palmitate and SCD1 inhibitor treatment caused substantial alterations in the PC/PE ratio. Disequilibrium in the proportion of these two most abundant membrane PLs was reported to negatively impact ER membrane integrity (56) and the response to stress stimuli (55, 57). Eventually, this might lead to a disruption of ER homeostasis, impairment of the unfolded protein response, and a reduction of insulin release. We observed these effects in INS-1E cells following simultaneous administration of the SCD1 inhibitor and palmitic acid. Therefore, our study demonstrates at least the partial requirement of ER stress in palmitate-derived lipotoxicity. Crosstalk between ER stress and the mitochondrial pathway is a well-documented phenomenon (56). A tempting speculation is that an increase

in cleaved caspase 9 levels, which was observed in our experimental model, reinforces this interaction. Mitochondria-driven apoptosis might also be induced by the accumulation of CL, together with an enhancement of its unsaturation associated with SCD1 inhibition. CL constitutes the main PL class of the mitochondrial inner membrane (36) and is extremely sensitive to damage that is caused by oxidative stress (57). In fact, mRNA level of lysophosphatidylcholine acyltransferase 3 (LPCAT3), a key enzyme responsible for a delivery of mature membrane PL by the remodeling pathway, was upregulated in HeLa cells with SCD1 knock-down and facilitated incorporation of PUFAs into the PL fraction, thus compensating for the decreased synthesis of MUFAs (52). Therefore, it is possible that LCLAT1, which is expressed in pancreas (58), increases upon SCD1 inhibition in INS-1E cells and leads to an abnormal CL remodeling, responsible for mitochondrial dysfunction and higher susceptibility to oxidative stress. In accordance with this, we saw a significant rise in the incorporation of linoleic acid, the main substrate of CL remodeling in all experimental groups when compared with BSA control (data not shown).

In conclusion, the present data provide evidence of a novel mechanism in which SCD1 operates as a metabolic link in the crosstalk between lipid toxicity, apoptosis, and autophagy in INS-1E cells. Based on these findings, we propose a model in which alterations in SCD1 activity modulate

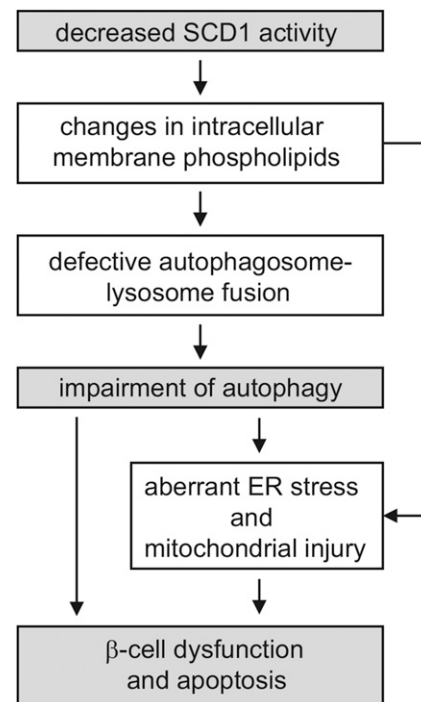



Fig. 8. Effect of SCD1 inhibition on palmitate-induced autophagy in INS-1E cells. A decrease in the activity of SCD1 changes the PL composition of cellular membranes and leads to defects in autophagic clearance because of impairments of autophagosome-lysosome fusion. Such prolonged stress interferes with ER function, which initiates mitochondrial collapse and apoptosis. Consequently, pancreatic β -cells exhibit decreases in insulin secretion and proliferation and finally cell death.

autophagy through aberrant autophagosome-lysosome fusion that is caused by changes in membrane PL saturation status, thus exacerbating the susceptibility of β -cells to palmitate-induced failure. Simultaneously, such structural alterations drive an ineffective ER stress response, which initiates mitochondrial apoptosis, a marked decrease in the functional capacity of β -cells, and finally cell death (Fig. 8). These responses are not mutually exclusive. Instead, they are intertwined in multiple ways. The activation of one response triggers another response, culminating in a cascade of damage. Inhibition of SCD was pointed out as a very promising strategy for the treatment of insulin resistance and obesity-related T2D (13). Nevertheless, the beneficial effects of systemic SCD1 inhibition on adiposity may occur at the expense of β -cells, possibly justifying a reconsideration of SCD inhibitors for T2D treatment and allowing the development of alternative therapeutic strategies. 

REFERENCES

- Prentki, M., and C. J. Nolan. 2006. Islet beta cell failure in type 2 diabetes. *J. Clin. Invest.* **116**: 1802–1812.
- Stein, D. T., B. E. Stevenson, M. W. Chester, M. Basit, M. B. Daniels, S. D. Turley, and J. D. McGarry. 1997. The insulinotropic potency of fatty acids is influenced profoundly by their chain length and degree of saturation. *J. Clin. Invest.* **100**: 398–403.
- Boucher, A., D. Lu, S. C. Burgess, S. Telemaque-Potts, M. V. Jensen, H. Mulder, M. Y. Wang, R. H. Unger, A. D. Sherry, and C. B. Newgard. 2004. Biochemical mechanism of lipid-induced impairment of glucose-stimulated insulin secretion and reversal with a malate analogue. *J. Biol. Chem.* **279**: 27263–27271.
- Busch, A. K., E. Gurisik, D. V. Corderly, M. Sudlow, G. S. Denyer, D. R. Laybutt, W. E. Hughes, and T. J. Biden. 2005. Increased fatty acid desaturation and enhanced expression of stearoyl coenzyme A desaturase protects pancreatic beta-cells from lipoapoptosis. *Diabetes*. **54**: 2917–2924.
- Biden, T. J., E. Boslem, K. Y. Chu, and N. Sue. 2014. Lipotoxic endoplasmic reticulum stress, beta cell failure, and type 2 diabetes mellitus. *Trends Endocrinol. Metab.* **25**: 389–398.
- Maechler, P. 2012. Mitochondrial signal transduction in pancreatic beta-cells. *Best Pract. Res. Clin. Endocrinol. Metab.* **26**: 739–752.
- Frigerio, F., T. Brun, C. Bartley, A. Usardi, D. Bosco, K. Ravnskjaer, S. Mandrup, and P. Maechler. 2010. Peroxisome proliferator-activated receptor alpha (PPARalpha) protects against oleate-induced INS-1E beta cell dysfunction by preserving carbohydrate metabolism. *Diabetologia*. **53**: 331–340.
- Maedler, K., G. A. Spinass, D. Dyntar, W. Moritz, N. Kaiser, and M. Y. Donath. 2001. Distinct effects of saturated and monounsaturated fatty acids on beta-cell turnover and function. *Diabetes*. **50**: 69–76.
- Hodson, L., and B. A. Fielding. 2013. Stearoyl-CoA desaturase: rogue or innocent bystander? *Prog. Lipid Res.* **52**: 15–42.
- Mauvoisin, D., and C. Mounier. 2011. Hormonal and nutritional regulation of SCD1 gene expression. *Biochimie*. **93**: 78–86.
- Ntambi, J. M., M. Miyazaki, J. P. Stoehr, H. Lan, C. M. Kendziorski, B. S. Yandell, Y. Song, P. Cohen, J. M. Friedman, and A. D. Attie. 2002. Loss of stearoyl-CoA desaturase-1 function protects mice against adiposity. *Proc. Natl. Acad. Sci. USA*. **99**: 11482–11486.
- Miyazaki, M., M. T. Flowers, H. Sampath, K. Chu, C. Ozelberger, X. Liu, and J. M. Ntambi. 2007. Hepatic stearoyl-CoA desaturase-1 deficiency protects mice from carbohydrate-induced adiposity and hepatic steatosis. *Cell Metab.* **6**: 484–496.
- Dobrzyn, P., M. Jazurek, and A. Dobrzyn. 2010. Stearoyl-CoA desaturase and insulin signaling—what is the molecular switch? *Biochim. Biophys. Acta*. **1797**: 1189–1194.
- Thörn, K., M. Hovsepian, and P. Bergsten. 2010. Reduced levels of SCD1 accentuate palmitate-induced stress in insulin-producing beta-cells. *Lipids Health Dis.* **9**: 108.
- Green, C. D., and L. K. Olson. 2011. Modulation of palmitate-induced endoplasmic reticulum stress and apoptosis in pancreatic beta-cells by stearoyl-CoA desaturase and Elovl6. *Am. J. Physiol. Endocrinol. Metab.* **300**: E640–E649.
- Flowers, J. B., M. E. Rabaglia, K. L. Schueler, M. T. Flowers, H. Lan, M. P. Keller, J. M. Ntambi, and A. D. Attie. 2007. Loss of stearoyl-CoA desaturase-1 improves insulin sensitivity in lean mice but worsens diabetes in leptin-deficient obese mice. *Diabetes*. **56**: 1228–1239.
- Singh, R., S. Kaushik, Y. Wang, Y. Xiang, I. Novak, M. Komatsu, K. Tanaka, A. M. Cuervo, and M. J. Czaja. 2009. Autophagy regulates lipid metabolism. *Nature*. **458**: 1131–1135.
- Liu, K., and M. J. Czaja. 2013. Regulation of lipid stores and metabolism by lipophagy. *Cell Death Differ.* **20**: 3–11.
- Ravikumar, B., S. Sarkar, J. E. Davies, M. Futter, M. Garcia-Arencibia, Z. W. Green-Thompson, M. Jimenez-Sanchez, V. I. Korolchuk, M. Lichtenberg, S. Luo, et al. 2010. Regulation of mammalian autophagy in physiology and pathophysiology. *Physiol. Rev.* **90**: 1383–1435.
- Fujitani, Y., T. Ueno, and H. Watada. 2010. Autophagy in health and disease. 4. The role of pancreatic beta-cell autophagy in health and diabetes. *Am. J. Physiol. Cell Physiol.* **299**: C1–C6.
- Jung, H. S., K. W. Chung, J. Won Kim, J. Kim, M. Komatsu, K. Tanaka, Y. H. Nguyen, T. M. Kang, K. H. Yoon, J. W. Kim, et al. 2008. Loss of autophagy diminishes pancreatic beta cell mass and function with resultant hyperglycemia. *Cell Metab.* **8**: 318–324.
- Ebato, C., T. Uchida, M. Arakawa, M. Komatsu, T. Ueno, K. Komiya, K. Azuma, T. Hirose, K. Tanaka, E. Kominami, et al. 2008. Autophagy is important in islet homeostasis and compensatory increase of beta cell mass in response to high-fat diet. *Cell Metab.* **8**: 325–332.
- Li, X., L. Zhang, S. Meshinchi, C. Dias-Leme, D. Raffin, J. D. Johnson, M. K. Treutelaar, and C. F. Burant. 2006. Islet microvasculature in islet hyperplasia and failure in a model of type 2 diabetes. *Diabetes*. **55**: 2965–2973.
- Gonzalez, C. D., M. S. Lee, P. Marchetti, M. Pietropaolo, R. Towns, M. I. Vaccaro, H. Watada, and J. W. Wiley. 2011. The emerging role of autophagy in the pathophysiology of diabetes mellitus. *Autophagy*. **7**: 2–11.
- Masini, M., M. Bugliani, R. Lupi, S. del Guerra, U. Boggi, F. Filipponi, L. Marselli, P. Masiello, and P. Marchetti. 2009. Autophagy in human type 2 diabetes pancreatic beta cells. *Diabetologia*. **52**: 1083–1086.
- Martino, L., M. Masini, M. Novelli, P. Befly, M. Bugliani, L. Marselli, P. Masiello, P. Marchetti, and V. De Tata. 2012. Palmitate activates autophagy in INS-1E beta-cells and in isolated rat and human pancreatic islets. *PLoS One*. **7**: e36188.
- Merglen, A., S. Theander, B. Rubi, G. Chaffard, C. B. Wollheim, and P. Maechler. 2004. Glucose sensitivity and metabolism-secretion coupling studied during two-year continuous culture in INS-1E insulinoma cells. *Endocrinology*. **145**: 667–678.
- Bligh, E. G., and W. J. Dyer. 1959. A rapid method of total lipid extraction and purification. *Can. J. Biochem. Physiol.* **37**: 911–917.
- Mei, S., H. M. Ni, S. Manley, A. Bockus, K. M. Kassel, J. P. Luyendyk, B. L. Copple, and W. X. Ding. 2011. Differential roles of unsaturated and saturated fatty acids on autophagy and apoptosis in hepatocytes. *J. Pharmacol. Exp. Ther.* **339**: 487–498.
- Khan, M. J., M. Rizwan Alam, M. Waldeck-Weiermair, F. Karsten, L. Groschner, M. Riederer, S. Hallström, P. Rockenfeller, V. Konya, A. Heinemann, et al. 2012. Inhibition of autophagy rescues palmitic acid-induced necroptosis of endothelial cells. *J. Biol. Chem.* **287**: 21110–21120.
- Barth, S., D. Glick, and K. F. Macleod. 2010. Autophagy: assays and artifacts. *J. Pathol.* **221**: 117–124.
- Mizushima, N., T. Yoshimori, and B. Levine. 2010. Methods in mammalian autophagy research. *Cell*. **140**: 313–326.
- Kim, E., J. H. Lee, J. M. Ntambi, and C. K. Hyun. 2011. Inhibition of stearoyl-CoA desaturase1 activates AMPK and exhibits beneficial lipid metabolic effects in vitro. *Eur. J. Pharmacol.* **672**: 38–44.
- Knaevelsrud, H., and A. Simonsen. 2012. Lipids in autophagy: constituents, signaling molecules and cargo with relevance to disease. *Biochim. Biophys. Acta*. **1821**: 1133–1145.
- Koga, H., S. Kaushik, and A. M. Cuervo. 2010. Altered lipid content inhibits autophagic vesicular fusion. *FASEB J.* **24**: 3052–3065.
- van Meer, G., D. R. Voelker, and G. W. Feigenson. 2008. Membrane lipids: where they are and how they behave. *Nat. Rev. Mol. Cell Biol.* **9**: 112–124.
- Listenberger, L. L., X. Han, S. E. Lewis, S. Cases, R. V. Jr Farese, D. S. Ory, and J. E. Schaffer. 2003. Triglyceride accumulation protects against fatty acid-induced lipotoxicity. *Proc. Natl. Acad. Sci. USA*. **100**: 3077–3082.

38. Tan, S. H., G. Shui, J. Zhou, Y. Shi, J. Huang, D. Xia, M. R. Wenk, and H. M. Shen. 2014. Critical role of SCD1 in autophagy regulation via lipogenesis and lipid rafts-coupled AKT-FOXO1 signaling pathway. *Autophagy*. **10**: 226–242.
39. Green, C. D., D. B. Jump, and L. K. Olson. 2009. Elevated insulin secretion from liver X receptor-activated pancreatic beta-cells involves increased de novo lipid synthesis and triacylglyceride turnover. *Endocrinology*. **150**: 2637–2645.
40. Hellems, K., K. Kerckhofs, J. C. Hannaert, G. Martens, P. Van Veldhoven, and D. Pipeleers. 2007. Peroxisome proliferator-activated receptor alpha-retinoid X receptor agonists induce beta-cell protection against palmitate toxicity. *FEBS J.* **274**: 6094–6105.
41. Hellems, K. H., J. C. Hannaert, B. Denys, K. R. Steffensen, C. Raemdonck, G. A. Martens, P. P. Van Veldhoven, J. A. Gustafsson, and D. Pipeleers. 2009. Susceptibility of pancreatic beta cells to fatty acids is regulated by LXR/PPARalpha-dependent stearyl-coenzyme A desaturase. *PLoS One*. **4**: e7266.
42. Ogasawara, Y., E. Itakura, N. Kono, N. Mizushima, H. Arai, A. Nara, T. Mizukami, and A. Yamamoto. 2014. Stearoyl-CoA desaturase 1 activity is required for autophagosome formation. *J. Biol. Chem.* **289**: 23938–23950.
43. Rubinsztein, D. C., T. Shpilka, and Z. Elazar. 2012. Mechanisms of autophagosome biogenesis. *Curr. Biol.* **22**: R29–R34.
44. Choi, S. E., S. M. Lee, Y. J. Lee, L. J. Li, S. J. Lee, J. H. Lee, Y. Kim, H. S. Jun, K. W. Lee, and Y. Kang. 2009. Protective role of autophagy in palmitate-induced INS-1 beta-cell death. *Endocrinology*. **150**: 126–134.
45. Menzies, F. M., K. Moreau, C. Puri, M. Renna, and D. C. Rubinsztein. 2012. Measurement of autophagic activity in mammalian cells. *Curr. Protoc. Cell Biol.* **Chapter 15**: Unit 15.16.
46. Tanida, I., N. Minematsu-Ikeguchi, T. Ueno, and E. Kominami. 2005. Lysosomal turnover, but not a cellular level, of endogenous LC3 is a marker for autophagy. *Autophagy*. **1**: 84–91.
47. Wu, Y. T., H. L. Tan, G. Shui, Ch. Bauvy, Q. Huang, M. R. Wenk, Ch. N. Ong, P. Codogno, and H. M. Shen. 2010. Dual role of 3-methyladenine in modulation of autophagy via different temporal patterns of inhibition on class I and III phosphoinositide 3-kinase. *J. Biol. Chem.* **285**: 10850–10861.
48. Dobrzyn, A., P. Dobrzyn, M. Miyazaki, H. Sampath, K. Chu, and J. M. Ntambi. 2005. Stearoyl-CoA desaturase 1 deficiency increases CTP: choline cytidyltransferase translocation into the membrane and enhances phosphatidylcholine synthesis in liver. *J. Biol. Chem.* **280**: 23356–23362.
49. Cnop, M., J. C. Hannaert, A. Hoorens, D. L. Eizirik, and D. G. Pipeleers. 2001. Inverse relationship between cytotoxicity of free fatty acids in pancreatic islet cells and cellular triglyceride accumulation. *Diabetes*. **50**: 1771–1777.
50. Le Lay, S., and I. Dugail. 2009. Connecting lipid droplet biology and the metabolic syndrome. *Prog. Lipid Res.* **48**: 191–195.
51. Borradaile, N. M., X. Han, J. D. Harp, S. E. Gale, D. S. Ory, and J. E. Schaffer. 2006. Disruption of endoplasmic reticulum structure and integrity in lipotoxic cell death. *J. Lipid Res.* **47**: 2726–2737.
52. Ariyama, H., N. Kono, S. Matsuda, T. Inoue, and H. Arai. 2010. Decrease in membrane phospholipid unsaturation induces unfolded protein response. *J. Biol. Chem.* **285**: 22027–22035.
53. Li, Z., L. B. Agellon, T. M. Allen, M. Umeda, L. Jewell, A. Mason, and D. E. Vance. 2006. The ratio of phosphatidylcholine to phosphatidylethanolamine influences membrane integrity and steatohepatitis. *Cell Metab.* **3**: 321–331.
54. Li, Y., M. Ge, L. Ciani, G. Kuriakose, E. J. Westover, M. Dura, D. F. Covey, J. H. Freed, F. R. Maxfield, J. Lytton, et al. 2004. Enrichment of endoplasmic reticulum with cholesterol inhibits sarcoplasmic-endoplasmic reticulum calcium ATPase-2b activity in parallel with increased order of membrane lipids: implications for depletion of endoplasmic reticulum calcium stores and apoptosis in cholesterol-loaded macrophages. *J. Biol. Chem.* **279**: 37030–37039.
55. Fu, S., L. Yang, P. Li, O. Hofmann, L. Dicker, W. Hide, X. Lin, S. M. Watkins, A. R. Ivanov, and G. S. Hotamisligil. 2011. Aberrant lipid metabolism disrupts calcium homeostasis causing liver endoplasmic reticulum stress in obesity. *Nature*. **473**: 528–531.
56. Malhotra, J. D., and R. J. Kaufman. 2011. ER stress and its functional link to mitochondria: role in cell survival and death. *Cold Spring Harb. Perspect. Biol.* **3**: a004424.
57. Li, J., C. Romestaing, X. Han, Y. Li, X. Hao, Y. Wu, Ch. Sun, L. S. Jefferson, J. Xiong, K. F. Lanoue, et al. 2010. Cardiolipin remodeling by ALCAT1 links oxidative stress and mitochondrial dysfunction to obesity. *Cell Metab.* **12**: 154–165.
58. Hishikawa, D., T. Hashidate, T. Shimizu, and H. Shindou. 2014. Diversity and function of membrane glycerophospholipids generated by the remodelling pathway in mammalian cells. *J. Lipid Res.* **55**: 799–807.